Peer-reviewed version available at Appl. Sci. 2020, 10, 1994; doi:10.3390/app10061994

Article

Exploring Geometric Feature Hyper-Space in Data to Learn Representations of Abstract Concepts

Rahul Sharma [1,‡], Bernardete Ribeiro [1] Alexandre Miguel Pinto [1,‡] and F. Amílcar Cardoso [1,]

[1] CISUC - University of Coimbra, Portugal; rahul@dei.uc.pt, bribeiro@dei.uc.pt, ampinto@dei.uc.pt, amilcar@dei.uc.pt

‡ These authors contributed equally to this work.

Abstract: The term Concept has been a prominent part of investigations in psychology and neurobiology where, mostly, it is mathematically or theoretically represented. The Concepts are also studied computationally through their symbolic, distributed and hybrid representations. The majority of these approaches focused on addressing concrete concepts notion, but the view of the abstract concept is rarely explored. Moreover, most computational approaches have a predefined structure or configurations. The proposed method, Regulated Activation Network (RAN), has an evolving topology and learns representations of Abstract Concepts by exploiting the geometrical view of Concepts, without supervision. In the article, the IRIS data was used to demonstrate: the RAN's modeling; flexibility in concept identifier choice; and deep hierarchy generation. Data from IoT's Human Activity Recognition problem is used to show automatic identification of alike classes as abstract concepts. The evaluation of RAN with 8 UCI benchmarks and the comparisons with 5 Machine Learning models establishes the RANs credibility as a classifier. The classification operation also proved the RAN's hypothesis of abstract concept representation. The experiments demonstrate the RANs ability to simulate psychological processes (like concept creation and learning) and carry out effective classification irrespective of training data size.

Keywords: unsupervised machine learning; hierarchical learning; computational representation; computational cognitive modeling; contextual modeling; classification; IoT data modeling

0. Introduction

Concepts are of great value to humans because they are one of the building blocks of our recognition process. They enable us to perform cognitive functions such as classification which is fundamental in decision making and also capacitate us for contextual comprehension. By definition, a concept refers to an 'idea' or a combination of several ideas but in the computational domain, a concept can be a feature (object or event) or set of features (objects or events). An individual concept is referred to as a concrete concept (or feature) whereas a generalized form of a set of concepts (or features) can be perceived as an abstract concept. There are several conceptual representation theoritical frameworks [1] like *modality-specific*, *localist-distributed*, *experience-dependent* [2].

In computational domain, the concepts are mostly represented by three broad categories i.e. symbolic (eg. ACT-R [3]), distributed (eg. ANN) and spatial (eg. Conceptual Space [4]) representations. Cognitive architecture like CLARION [5] is an example of a hybrid computational representation that combines symbolic and distributed approaches, but there is no hybrid approach that combines all the three representations. Moreover, the symbolic, distributed, spatial and hybrid (spatial+distributed) representations are mostly used on representing concrete concepts (like object detection) whereas the notion of an abstract concept is debated [1] but rarely explored.

Preprints (www.preprints.org) | NOT PEER-REVIEWED | Posted: 31 January 2020 doi:10.20944/preprints202001.0375.v1

Peer-reviewed version available at Appl. Sci. 2020, 10, 1994; doi:10.3390/app10061994

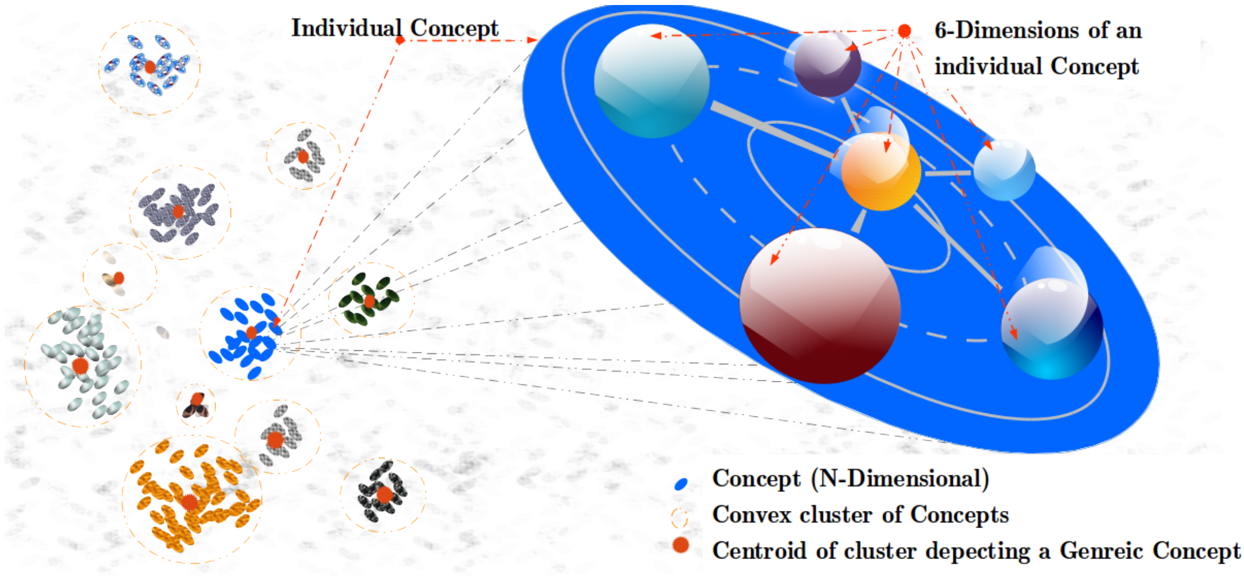

Figure 1. A universe of Concepts in six-dimensional feature hyper-space. The ovals in the diagram depict individual Concepts. Each *individual Concept* is described by their defining 6-dimensions. The cluster of Concepts shows the groups formed by similar Concepts represented by a *Convex cluster of Concepts*, and the *cluster centers* depicts the most generic Concept of the cluster.

This article proposes a computational method named Regulated Activation Network (RAN) which unifies the virtues of symbolic, distributed and spatial representations to represent concepts (both concrete and abstract). RAN has a graph-based topology hence it is distributed, every node in the graph (network) identifies an entity, therefore, it's symbolic, and every node (or entity) is viewed in an n-dimensional feature space, hence, it's also spatial. The spatial view of concepts as points in multidimensional geometric feature space (see Figure 1 for 6-dimensional View of Concepts) is inspired by the theory of conceptual spaces [4]. The RAN's modeling has an evolving topology that enables it to build a model depicting a hierarchy of concepts. The geometrical associations among concepts aid in determining the Convex Abstract Concepts. Further, the representatives (nodes) of the Abstract Concepts form a new layer dynamically, where each node acts as a Convex Abstract Concept representative for the underlying category. Symbolically, the concepts at (relatively) lower level in the hierarchy are identified as concrete concepts and the concepts at (relatively) higher level are seen as abstract concepts.

The model generation process with RAN and the three cognitive functions (i.e. concept creation, learning and activation propagation) are simulated using a IRIS data. The deep hierarchy generation, automatic generic concept modeling simulations are performed using 2 UCI benchmark: IRIS data; and IoT data from smartphone sensors. The application of RAN as a classifier is reported along with the proof of concept of classification using 8 UCI benchmark datasets. The generated models were evaluated using metrics precision, recall, F1-score, accuracy and Receiver Operating Characteristic (ROC) curve analysis. The article also reports the RANs classification and feature comparison with five machine learning techniques, Multilayer Perceptron (MLP) [6], Logistic Regression (LR) [7], K Nearest Neighbors (K-NN) [8], Stochastic Gradient Descent (SGD) [9] and Restrict Boltzmann Machine [10] pipelined with Logistic Regression (RBM+).

The article is organized in the following order; Section 1 puts forward the work closely related to Abstract Concept representation and models with evolving topology. Section 2 describes the background associated with principles, theories, and motivations for RAN's modeling. RANs methodology is detailed using a IRIS data in Section 3. Section 4 shows the experiments with two datasets acquired from UCI machine learning repository to exhibit *(1)* flexibility in choosing a suitable concept identifier, *(2)* building a deep hierarchy of Abstract Concepts, *(3)* automatic association of

Preprints (www.preprints.org) | NOT PEER-REVIEWED | Posted: 31 January 2020 doi:10.20944/preprints202001.0375.v1

Peer-reviewed version available at Appl. Sci. 2020, 10, 1994; doi:10.3390/app10061994

input-labels to their respective Abstract Concept nodes. Section 5 provides RANs comparisons with five classifiers and proof of concept with eight benchmark datasets. At last, Section 6 summarizes and concludes the article with remarks over ongoing and future work.

1. Related Work

Abstract Concepts are of immense value because they help in developing unique abilities in humans such as relative recognition and effective decision-making. In medical science, there have been significant efforts to study Abstract Concepts with the help of technology. One such example is MRI[1], which is being used to inspect the sections of the brain involved in Abstract Concept identification [11, 12]. Research in psychology has also reported investigations over Abstract Concepts, like probing the role of emotional content in processing and representing Abstract Concepts [13].

There has been a notable contribution from cognitive, and psycholinguists in studying languages through Abstract Concept modeling and representations. Internally representing Abstract Concepts via amodal symbols like a feature list, and frames [14,15] is among the preliminary research work in linguistics. The association and context were also established, to relating Abstract and Concrete words [14]. Some research reveals that we internally recognize metaphors as Abstract Concepts [16]. Besides theoretical methods, computational approaches are playing a vital role in comprehending and representing Abstract Concepts. Research in NLP addresses computational learning, comprehension and processing of human understandable language, and its components. An interesting article published a work about the representation of Abstract, and Concrete Concepts in daily written Language using a text-based multimodal architecture of NLP [17]. Other than NLP, semantic networks are also used to study semantic similarity among Abstract, and Concrete nouns (of Greek, and English) [18] with the aid of network-based Distributed Semantic Model [19].

Though the aforementioned computational approaches contribute toward Abstract Concept modeling and representation, they have a fixed topology (i.e., the modeling process begins with a fixed structure and configuration). In connectionist computational modeling, there have been efforts to develop models that evolve. ANNA ELEONORA (standing for Artificial Neural Networks Adaptation: Evolutionary LEaming Of Neural Optimal Running Abilities) [20] demonstrated a way to grow neural networks with the aid of parallel genetic algorithms. NEAT (NeuroEvolution of Augmenting Topologies) [21] is another work that reported evolving neural network modeling, showing how nodes and weights are added to the model when new features emerge as part of the existing population and CoDeepNEAT [22] is the most recent member of such evolving models. Markov Brains [23] also belong to the family of evolving neural networks which uses binary variables and arbitrary logic to implement deterministic or probabilistic finite state machines. They have been used to investigate behaviors, character recognition and game theory.

This article communicates an approach which is not only hybrid but also has an evolving topology. The RANs modeling learns the representation of the Convex Abstract Concepts dynamically, hence makes it an evolving topology. RANs approach is connectionist, and each newly created node corresponds to an Abstract Concept symbolically, thus portraying its hybrid characteristics.

2. Background

This section provides information about the principles and methodologies related to RANs modeling. It highlights the significance of each approach, along with their applicability in RANs modeling.

---

[1] Magnetic Resonance Imaging

Preprints (www.preprints.org) | NOT PEER-REVIEWED | Posted: 31 January 2020 doi:10.20944/preprints202001.0375.v1

Peer-reviewed version available at Appl. Sci. 2020, 10, 1994; doi:10.3390/app10061994

2.1. Principles of Regulated Activation Networks

The tenets of RANS modeling, presented in [24], states model should be topologically a connectionist and intends to represent and simulate the dynamic cognitive state of an agent. In the first version RANs [24] the authors implemented a single-layer version of the model where each node had a lateral connection to its same-layer companions. It had a simple learning and reasoning mechanisms, but these showed to be sufficient to simulate several known cognitive phenomena such as the Priming [25], the False Memory [26,27].

Two principles of Regulated Activation Networks inspired our proposal. First, the model should be dynamic, and this is achieved by dynamically creating layers (deep representations) of Concepts. Second, the model must be capable of learning and creating an Abstract representation of Concepts. This is obtained by viewing associations among the Concepts (at the same level) in n-dimensional geometric space, and learning relationship between the newly created Abstract Concepts, and input level Concepts.

2.2. Conceptual Spaces

Conceptual Spaces theory [4] is one of the cognitive approaches that form the basis of RANs modeling. This theory views the Concepts as regions within a multi-dimensional space, with the data features representing the dimensions. The *similarity* among the Concepts can be identified based upon the geometrical distance between the objects. The Conceptual Spaces, thus, serves as a natural way or tool to capture the similarity relationships among Concepts, or Objects. Under this setting, one data instance corresponds to a single point in the space. Formally we can say, the *Quality Dimensions*, i.e., a set of $D_1, \ldots., D_n$, forms the Conceptual Space S. A point in S is represented by a vector $v = \langle d_1, \ldots., d_n \rangle$, where *{1,....n}* are the indexes of the dimensions. Atomic Concepts are Convex Regions –a Convex Region C having point x that falls between points $x_1 \in C$ and $x_2 \in C$ also belongs to C. The quality dimension is the basic requirement for Conceptual Spaces [28]. An example is a color space with the dimensions Hue, Saturation, and Brightness. Each quality dimension has a geometrical structure. For example, Hue is circular, whereas brightness and saturation correspond with finite linear scales (see Figure 2).

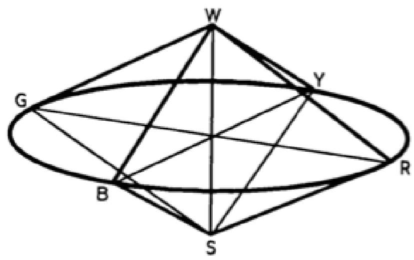

Figure 2. The color space [29]

The theory of Conceptual Spaces also addresses *prototype theory* of categorization [30–32]. The main idea of prototype theory is that within a category of objects, like those instantiating a Concept, certain members are judged to be more representative of the group than others. For example, robins are judged to be more representative of the category "bird" than are ravens, penguins, and emus. If Convex Regions of Conceptual Space describes Concepts, then prototype effect is, indeed, expected, i.e., the most likely central position of a Convex Region describes an Abstract Concept. For example, if color Concepts in a Convex region identified as subsets of the color space, then the central points of these regions would be the most prototypical examples of the color.

Clustering is a suitable way of identifying and learning atomic Convex Concepts in conceptual spaces. There are several clustering techniques, like hierarchical clustering, subspace clustering [33], partitioning relocation clustering, density-based clustering, grid-based clustering and many more.

Preprints (www.preprints.org) | NOT PEER-REVIEWED | Posted: 31 January 2020 doi:10.20944/preprints202001.0375.v1

Peer-reviewed version available at *Appl. Sci.* **2020**, *10*, 1994; doi:10.3390/app10061994

Table 1. Notations

Notation	Description
W	Inter-Layer weight matrix
A	Output Activation
a	Input Activation
n_a	Number of elements in input vector at Layer l
n_A	Number of elements in output vector at Layer $l+1$
l	l'th Layer representative
d	Normalized Euclidean distance
C	Cluster center or Centroids
i, j, k	Variables to represent node index for input-level, abstract-level, and arbitrary node index in either of the levels, respectively
t	Iterator variable
$f(x)$	Transfer function to obtain similarity relation

Many are frequently used in the statistical and scientific analysis of data [34,35], and in machine learning for the identification of Concepts/features [36]. On the other hand, the creation of a hierarchy of sub/super-Concepts is a way to represent more Abstract Concepts and their taxonomic-like relations. Deep learning techniques [37–40,40,41] found in the literature can also be used to create deep hierarchical representations, but usually do not interpret data as points in Conceptual Spaces. In the proposed approach, the clustering techniques enable us to identify categories of Concepts in a Conceptual Space thus laying the foundation to form a layer of Abstract representation of Concepts.

2.3. Spreading Activation

Spreading Activation is a theory of memory [42] based on Collins and Quillian's computer model [43] which has been widely used for the cognitive modeling of human associative memory and in other domains such as information retrieval [44]. It intends to capture the information representation and how it is processing. According to the theory, long-term Memory is represented by nodes and associative links between them, forming a semantic network of Concepts. The links characterized by a weight denotes the associative or semantic relation between the Concepts. The model assumes activating one Concept implies the spreading of activation to related nodes, making those memory areas more available for further cognitive processing. This activation decays over time as it spreads, which can occur through multiple levels [45], and the further it gets the weaker it becomes. That is usually modeled using a decaying factor for activation. The method of spreading activation has been central in many cognitive models due to its tractability and resemblance of interrelated groups of neurons in the human brain [46]. This theory of Spreading Activation inspires the activation propagation mechanism in our proposal to propagate (spread) activation in the upward direction, i.e., from the input-to-abstract layer in the network. The method has its significance, i.e., in the creation of the network, and in understanding the created Abstract Concepts.

3. Abstract Concept Modeling with RANs

The data value used with RANs modeling should be between "0" and "1" (both inclusive). This limitation has its inspiration from biological neurons, a value "0" indicates neuron (or node) is inactive, whereas "1" shows the neuron is highly active. An additional header is also needed for modeling with RAN. The size of the header is the same as the dimension of the input data vector, and each header element holds the largest value of their corresponding input data attribute. See Section A.1 for elaboration. RANs works with multivariate datasets except image because pictures are not ideal

doi:10.20944/preprints202001.0375.v1

Peer-reviewed version available at *Appl. Sci.* **2020**, *10*, 1994; doi:10.3390/app10061994

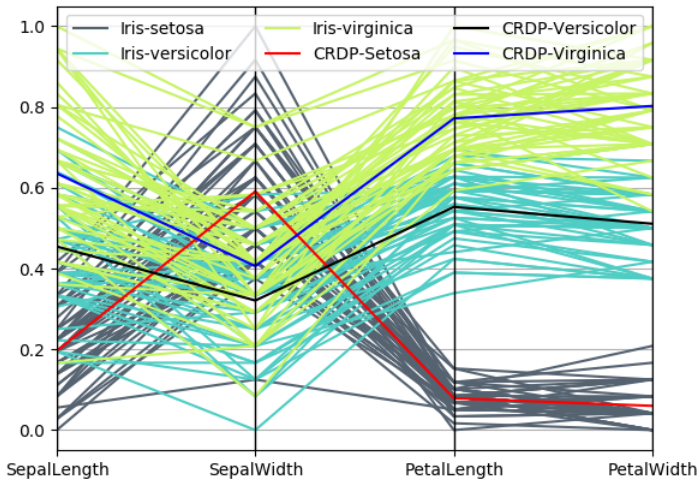

Figure 3. Parallel coordinate plot of normalized IRIS data. The plot shows the three classes of IRIS data along with their Cluster Representative Data Points (CRDP).

candidates to be interpreted as points in conceptual spaces, (discussed in Section 2.2). For this reason, our approach will, most probably, underperform on image processing tasks against other models that are, individually, designed for this kind of data, such as deep representations built with Convolutional Networks [40,47,48]; our technique is preferably suitable for understanding and simulating cognitive processes like Abstract Concept Identification.

The proposed approach models Convex Abstract Concepts through four core steps (i.e., *Concept Identification, Concept Creation, Interlayer Learning and Upward Activation Propagation*), along with one optional step (i.e., *Abstract Concept Labeling*). The RAN's methodology is explained using benchmark IRIS dataset. Figure 3 shows the parallel coordinate plot of IRIS data normalized between [0, 1] using min-max technique. The plot also shows the Cluster Representative Data Points (CRDPs) for all three classes of IRIS data (the importance of CRDP is detailed in 3.1). The objective of this experiment is to show how RANs build a hierarchical representation dynamically and simulate cognitive process of *concept creation*, *learning*, and *activation propagation*. For this experiment, it was hypothesized that the created abstract concepts symbolically represents the three classes of IRIS data. Classification operations were performed to prove the hypothesis which are reported at the end of this section.

3.1. Step 1: Concept Identification (CI) Process

The concept identification is the process of identifying convex groups in the input data. This is realized by categorizing the input data based upon their geometrical relationship, i.e., distance, conforming to the theory of conceptual spaces (see Section 2.2). The quality-dimension (i.e. SepalLength, SepalWidth, PetalLength and PetalWidth attributes of input data) symbolically represents input nodes (i.e. S_1, S_2, S_3 and S_4 see Figure 4). In this experiment, K-means [49] clustering method is used a concept identifier and applied to determine the convex groups in the IRIS data. The K-means was configured to determine the 3 classes (i.e. Iris-setosa, Iris-virginica, and Iris-Versicolor) of IRIS data. The clustering operation also determines the three cluster centers as Cluster Representative Data Points (CRDPs). According to the theory of prototype (see Section 2.2) these three CRDPs are the most probable representative of the three convex groups respectively, therefore are of great importance in learning relationship among concepts in two adjacent layers (see Section 3.3).

Any clustering algorithm can act as a Concept Identifier in RANs modeling if it suffices two basic requirements. First, the algorithm is able to determining Convex categories based upon their geometric relationship among the data instances. Second, the algorithm recognizes CRDPs of all the

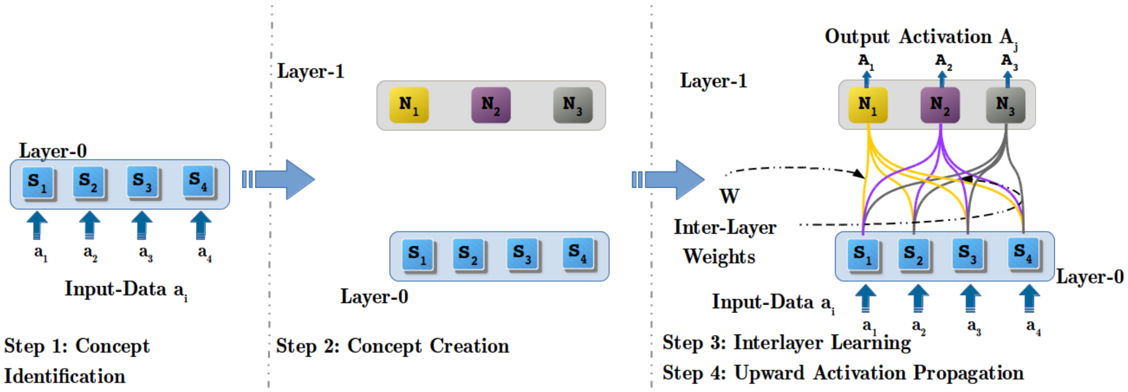

Figure 4. Steps in model generation with Regulated Activation Networks. The nodes S_1, S_2, S_3 and S_4 symbolically represents SepalLength, SepalWidth, PetalLength and PetalWidth attributes of input data.

identified clusters. This flexibility of choosing a suitable method for Concept Identification process in RANs modeling is demonstrated by a separate experiment using Affinity propagation [50] clustering algorithm, in Section 4.1.

3.2. Step 2: Concept Creation (CC) Process

Concept creation is a cognitive process to create representation of a newly identified concept. In RANs this cognitive process is simulated by creating a new layer of concepts dynamically. Each constituent node in the new layer symbolically acts as an abstract representative of their respective categories identified in the CI process. Step-2 in Figure 4 shows the newly created layer (Layer-1), that has 3 nodes (N_1, N_2 and N_3), corresponding to 3 classes (i.e. Iris-setosa, Iris-virginica, and Iris-Versicolor) of IRIS data (see Figure 3), identified in CI operation.

3.3. Step 3: Inter-Layer Learning (ILL) Process

Learning is an important cognitive process it acts as a relationship to associate concepts. In RANs modeling, learning is simulated by an assignment operation. As aforestated in Section 3.2 that each node in the new layer is an Abstract representative of categories identified in CI process, thus we learn association among the two-layer such that it substantiates the Abstract representation by the nodes at the new layer. Since CRDPs (see Section 3.1) are the most apparent choice as an Abstract representative of a cluster (and adhere to the inspiration from prototype theory); consequently, the CRDPs assigned as an association between the two layers.

Equation 1 shows the general learning in the form of a matrix, where W is the learned Inter-Layer Weight (ILW) between node j at new layer (i.e., Layer-1 in Figure 4) and node i at input layer (i.e., Layer-0). The set of ILWs, from one node j at new layer to all input nodes i, are the values of CRDP of j^{th} cluster center (i.e., C_j) identified in CI process. For instance, cluster center C_1 (see Figure 3) forms the weight vector [$W_{1,1}$, $W_{1,2}$, $W_{1,3}$ and $W_{1,4}$] (ILWs shown by 4 yellow lines in Step 3 Figure 4) between the node N_1 at Layer-1 and all four input nodes S_1, S_2,S_3 and S_4 at Layer-0.

$$W = \begin{bmatrix} W_{1,1}, W_{1,2}, \ldots, W_{1,n_a} \\ \ldots \\ W_{k,1}, W_{k,2}, \ldots, W_{k,n_a} \\ \ldots \\ W_{n_A,1}, W_{n_A,2}, \ldots, W_{n_A,n_a} \end{bmatrix} = \begin{bmatrix} C_1 \\ \ldots \\ C_k \\ \ldots \\ C_{n_A} \end{bmatrix} \tag{1}$$

Where j=1, 2, ..., n_A, and i=1, 2, ..., n_a.

Preprints (www.preprints.org) | NOT PEER-REVIEWED | Posted: 31 January 2020 doi:10.20944/preprints202001.0375.v1

Peer-reviewed version available at *Appl. Sci.* **2020**, *10*, 1994; doi:10.3390/app10061994

3.4. Step 4: Upwards Activation Propagation (UAP) Process

This upward activation propagation is a geometric reasoning operation, i.e., a non-linear projection of an i-dimensional input data vector a_i, into a j-dimensional output vector A_j (see Step 4 in Figure 4). The UAP operation is carried out in two stages, in the first stage the geometric distance operation takes place, and in the second stage, geometric distance is translated to establish a similarity relation.

3.4.1. Geometric Distance Function (GDF)- Stage 1

In the first phase of the UAP mechanism we determine the geometrical distance between the learned weight vectors (see Equation 1) and an input instance a_i. The numerator of Equation 2 shows a function to calculate the Euclidean distance between the jth weight vector and input vector a_i. The denominator of Equation 2 shows the relation that normalizes[2] the calculated distance between [0, 1].

$$d_j = \frac{\sqrt{\sum_{i=1}^{n_a}(W_{j,i} - a_i)^2}}{\sqrt{n_a}} \tag{2}$$

And consequently, j normalized Euclidean distances d_j are obtained between all j weight vectors and input instance a_i.

3.4.2. Similarity Translation Function (STF)- Stage 2

In the second phase the calculated normalized distance is transformed to obtain a similarity relation such that following requirements are fulfilled:

- $f(d = 0) = 1$, i.e. when distance is 0 similarity is 100%.
- $f(d = 1) = 0$ i.e. when distance is 1 similarity is 0%.
- $f(d = x)$ is continuous, monotonous, and differentiable in the $[0, 1]$ interval.

$$f(x) = (1 - \sqrt[3]{x})^2 \tag{3}$$

In RANs modeling Equation 3 is used as the Similarity Translation Function to determine the similarity relation of the previously calculated distance. The non-linearity of STF is depicted in Figure 5, indicating that the similarity value reduces drastically when the normalized Euclidean distance is larger than 0.05 (or 5% dissimilar).

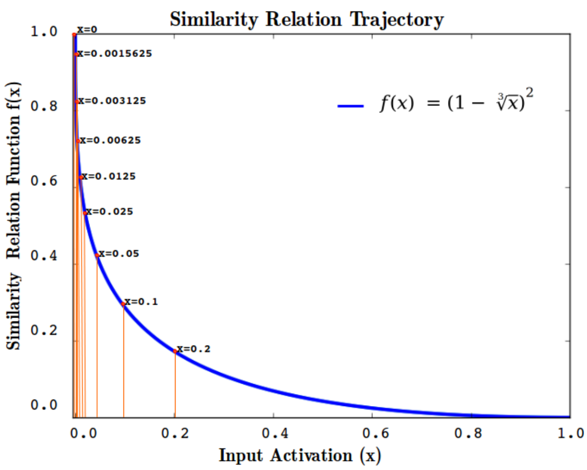

Figure 5. Plot of Similarity Translation Function with respect to varying input values in range $[0, 1]$

[2] In RANs modeling the activation values are, by definition, real values in the $[0, 1]$ interval – in an n-dimensional space the maximal possible euclidean distance between any two points is $\sqrt{\sum_{i=1}^{n}(a_i - 0)^2}=\sqrt{n}$, where a_i=1.

Preprints (www.preprints.org) | NOT PEER-REVIEWED | Posted: 31 January 2020 doi:10.20944/preprints202001.0375.v1

Peer-reviewed version available at Appl. Sci. 2020, 10, 1994; doi:10.3390/app10061994

Algorithm 1 Upwards Activation Propagation algorithm

Input: Vector $[a_1, a_2, ..., a_{n_a}]$ as input at layer l.

Output: New activation vector $[A_1, A_2, ..., A_{n_A}]$ in layer $l+1$.

for Each node A_j in layer $l+1$ **do**

Calculate Normalized Euclidean Distance:

$d_j = \frac{\sqrt{\sum_{i=1}^{n_a}(W_{j,i}-a_i)^2}}{\sqrt{n_a}}$

Transform d_j through STF Equation 3:

$A_j = f(d_j^2)$

end for

Where:

i= $[1, 2, ..., n_a]$.

j= $[1, 2, ..., n_A]$.

$W_{j,i}$ is ILW see Equation 1.

The first three steps generate the RANs model (see Figure 4), later, in the fourth step, this model is used via UAP operation by propagating the input activation (a_i) upward and obtaining activation (A_j) at Convex Abstract Concept layer (inspired by the theory of spreading activation see Section 2.3). Algorithm 1 describes the Upward Activation Propagation operation, showing how the inputs and interlayer learning weights W are used to calculate similarity relation to generating output activation at each Abstract Concept representative nodes. The activation A_j in newly created nodes N_j also indicate the degree of confidence (DoC) of the identification of a class by its representative node in the new layer (for a given input data instance). For instance, in Figure 4, Step-2, at Layer-0 input vector is [0.1, 0.21, 0.12, 0.5] it signifies that the dimensions S_1, S_2, S_3 and S_4 has activation 0.1, 0.21, 0.12, and 0.5 respectively. For the, aforementioned, input vector, [0.13, 0.32, 0.89] vector of activation is observed at all nodes (N_1, N2 and N_3) respectively, at Layer-1. The observed activation vector itself describes that the input data belongs to Class-3 (Versicolor) with a DoC of 89%.

3.5. RANs Proof of Hypothesis

In the beginning of this Section 3 it was hypothesized that nodes in the newly created layer symbolically represents abstract concepts of the 3 classes (Iris-setosa, Iris-virginica and Iris-versicolor) of Iris data. This hypothesis can be proven through classification operation using the RAN model generated with IRIS data. The classification experiment setup consists of 30 iterations of an experiment. Each experiment consist of 9 Research Design (RD)(see Table A3 in Section A.2), where, in every RD a 10-fold cross-validation procedure was applied. To carry out the evaluation operation *True-labels*, and *Test-labels* are determined via Abstract Concept Labeling (ACL) operation of RANs (see Section A.4 for ACL's description). Further, these labels were used to form a multi-class confusion matrix for the 3 classes of IRIS data. and with the aid of this confusion matrix 4 metrics (i.e. Precision, Recall, F1-Score, and Accuracy) were calculated.

Multi-class Receiver Operating Characteristics (ROC) curves were also plotted for the 3 classes to support the classification experiment with IRIS data. The binary labels corresponding to the True-labels (obtained via ACL operation) were obtained using the method node-wise binary transformation of input True-label (see Section A.3). Further, the confidence scores for the binary vectors were calculated using the node-wise confidence-score calculation method (described in Section A.3).

The Table 2 not only shows the RAN's comparison with other 5 classifiers but also that RAN indeed preformed well in the classification process with a performance of 95% (ca.) for all classification

Preprints (www.preprints.org) | NOT PEER-REVIEWED | Posted: 31 January 2020 doi:10.20944/preprints202001.0375.v1

Peer-reviewed version available at Appl. Sci. 2020, 10, 1994; doi:10.3390/app10061994

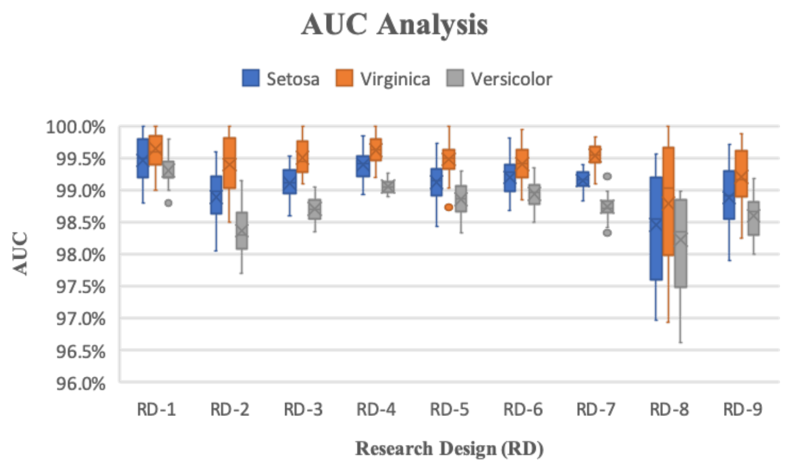

Figure 6. Area Under Curve for the 3 classes of IRIS for nine Research Designs (RD) of varying Test and Train data sizes

Table 2. RAN's classification study with IRIS data

Model	Precision (%)	Recall (%)	F1-Score (%)	Accuracy (%)
RBM	79.81 ±11.91	77.41 ±11.88	70.66 ±16.28	77.41 ±11.88
K-NN	90.41 ±28.77	92.8 ±21.61	91.00 ±27.01	92.80 ±21.61
LR	97.38 ± 4.15	96.64 ± 5.65	96.45 ± 6.12	96.64 ± 5.65
MLP	97.31 ± 0.71	96.86 ± 1.13	96.81 ± 1.21	96.86 ± 1.13
RANs	95.42 ± 0.67	95.02 ± 0.94	94.98 ± 0.98	95.02 ± 0.94
SGD	94.47 ± 6.40	94.46 ± 5.20	93.31 ± 6.78	94.46 ± 5.20

metrics. The ROC curve analysis also observed an Area Under Curve (AUC) of 99.07% (ca.), 99.40% (ca.) and 98.75% (ca.) for IRIS Setosa, Virginica and Versicolor classes respectively. These results shows the ability of RAN's modeling to identify the abstract concept where the three nodes (N_1, N_2 and N_3) in Layer-1 symbolically represents the classes IRIS Setosa, Virginica and Versicolor, respectively, as abstract concepts, hence proves the hypothesis.

4. Behavioral Demonstration of RANs

This section exhibits two distinct aspects of RANs modeling via separate experiments. Both investigations present a different view of RANs methodology, highlighting the capabilities of the RANs approach.

4.1. Experiment with IRIS dataset

There are two objectives of this probe, first is to demonstrate flexibility in choosing an appropriate methodology for Concept Identification operation in RANs modeling (see Section 3.1). Second is to show how RANs modeling can be used to build a deep hierarchy of Convex Abstract Concepts dynamically. This experiment uses Affinity propagation [50] clustering algorithm as a Concept Identifier to support the claim of independence in selecting a suitable clustering method for CI process in RANs modeling. Unlike the K-means algorithm (used to describe the RANs methodology in Section 3), with the Affinity Propagation algorithm, the number of clusters within the data need not be known beforehand. Furthermore, Affinity Propagation conforms to the basic requirements (see Section 3.1) for being a Concept Identifier in RANs modeling.

The second prospect of this experiment is to illustrate the dynamic topology of RANs approach where the network grows to form several layers representing Convex Abstract Concepts. For this demonstration, an algorithm is developed, named Concept Hierarchy Creation (CHC) algorithm (see 2). The CHC algorithm streamlines all four steps of RANs modeling (i.e., CI, CC, ILL and UAP)

Peer-reviewed version available at Appl. Sci. 2020, 10, 1994; doi:10.3390/app10061994

and uses these steps iteratively to build a hierarchy of Convex Abstract Concepts as described through Algorithm 2. This experiment was also conducted using the IRIS dataset obtained from the UCI machine learning repository [51]. In the CHC algorithm the Affinity propagation clustering algorithm was initialized with the following parameters: (1) damping_factor (DF) = 0.94 for layers below level 3, DF = 0.9679 for the layers at level 3 and above; (2) convergence_iteration=15; (3) max_iteration=1000.

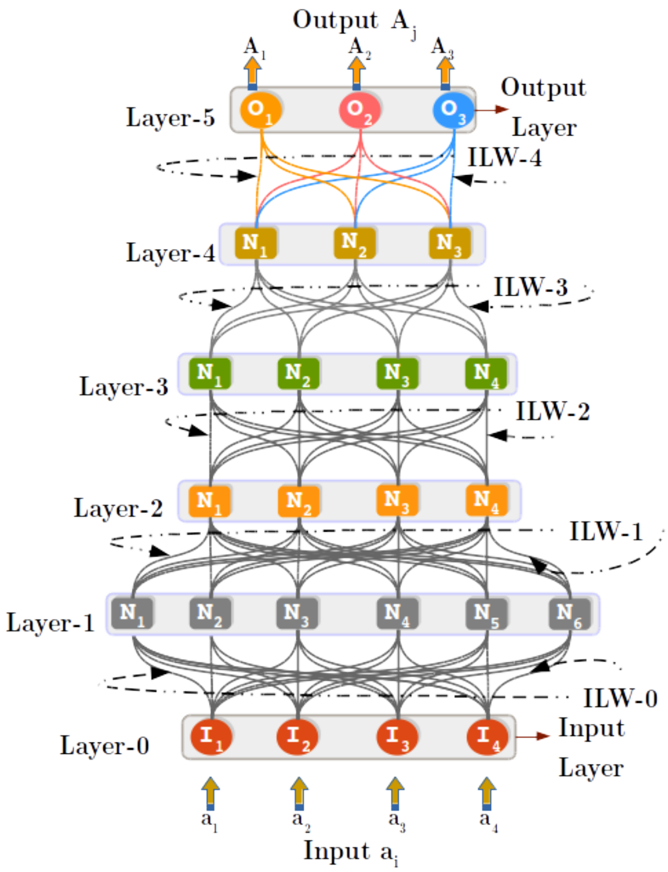

Figure 7. The model generated with 90% stratified IRIS data using Concept Hierarchy Creation Algorithm. Layer-0 is created while initializing the CHC algorithm. The algorithm grew to a *Desired-depth* of six Layers (including input Layer-0), and in each iteration of CHC algorithm a new layer is created dynamically and the Interlayer weights (ILW) are learned between the existing layer and a newly created layer above it.

Input layer-0 was created, with four nodes (equal to the dimension of IRIS data), and the RANs hierarchy generation is carried out according to Algorithm 2. The model obtained from CHC process is depicted by Figure 7, the model was initialized to grow six layers deep. Therefore, hierarchy augmentation terminates at Layer-5, with Layer-5 identified as most Abstract layer consisting of three nodes acting as Abstract representatives of three categories of flowers of IRIS dataset. To evaluate the obtained RANs model, *True-labels*, and *Test-labels* were retrieved using an Abstract Concept labeling procedure (see Section A.4). A confusion matrix (see Figure 8) was generated using the True and Test labels. With the aid of the confusion matrix, Precision, Recall, F1-Score and Accuracy were calculated to evaluate the model. The model performed quite decently with an observed accuracy of 93.33 (ca.), the results of precision, recall and F1-Score are reported in Table 3. The ROC curve analysis of the RANs model, as shown in Figure 9, displays the various operating characteristic and the observed Area Under Curve for all the classes of IRIS data. In this experiment, it is worth mentioning the application of RANs modeling for data dimension transformation and data visualization. In Figure 7 we can observe that the dimension of Layer-0 is four, whereas the size of the other layers either expands or reduces when the network grows. This dimension transformation operation is helpful in addressing

Preprints (www.preprints.org) | NOT PEER-REVIEWED | Posted: 31 January 2020 doi:10.20944/preprints202001.0375.v1

Peer-reviewed version available at Appl. Sci. 2020, 10, 1994; doi:10.3390/app10061994

Algorithm 2 Concept Hierarchy Creation Algorithm

Input: Multi-variate data with values between [0,1].
Output: Set of layers of Concepts – concept hierarchy.

Initialization: Create input layer layer-0 having dimension equal to that of input data.
Set *Current-layer-size* $CLS = i$, dimension of *input-data* vector.
Set *Layer-count* L= 0.
Set *Desired-depth*= 6.
Select Clustering algorithm and initialize.
Set *current-data* = *input-data*.
repeat
  Run *clustering algorithm* on *current-data* to identify set of cluster centers C.
  Create a *new-layer* above *current-layer*, with no nodes.
  for each cluster center $C_j \in C$ **do**
    Create new node j in *new layer l+1*.
    for each node i in *current-layer* **do**
      Create a new weighted connection $W_{c_j,i}$ between c_j and i such that $W_{c_j,i}$ is the coordinate of c along the i dimension.
    end for
  end for
  Set *new-data* = empty data set.
  for each *datum* in *current-data* **do**
    Inject *datum* in *current-layer*
    Propagate activation from *current-layer* to *new-layer* using algorithm 1.
    Add activation pattern produced in *new-layer* to *new-data*.
  end for
  Set $L = L + 1$.
  Set CLS = number of clusters in *current-layer*.
  Set *current-data* = *new-data*.
  Set *current-layer* = *new-layer*.
until CLS=1 **OR** *Desired-depth*= L.

		Predicted Labels: Class-0	Class-1	Class-2	
True label	Class-0	100%	0%	0%	5
	Class-1	0%	100%	0%	5
	Class-2	0%	20%	80%	5
		5	6	4	15

Figure 8. Confusion Matrix generated to validate RANs model with IRIS data (having 9 : 1 *train, and test* data ratio) for Class-0 (Setosa), Class-1 (Verisicolour), and Class-2 (Virginica).

the issue of the cures of dimensionality. Besides, the transformed data can be plotted to extract useful information from the data.

4.2. Experiment with Human Activity Recognition Data

This experiment aims to show the ability of the RANs approach to build the representation of generic Concepts. The experiment uses UCIHAR [52] dataset for home activity recognition using the smartphone, obtained from the UCI machine learning repository. The data captured six activities Walking, Walking_upstairs, Walking_downstairs, Sitting, Standing, and Laying. The hypothesis of this experiment is that the labels Walking, Walking_upstairs, Walking_downstairs are identified by an abstract concept (say) *Mobile* and the other 3 labels Sitting, Standing, and Laying by abstract concept (say) *Immobile*. In this experiment also classification operation can be used to prove the hypothesis.

The UCIHAR dataset was normalized and a header was attached. In CHC algorithm K-means is chosen as concept identifier and the parameter *Desired-depth* was set to 1 so that model has only

Preprints (www.preprints.org) | NOT PEER-REVIEWED | Posted: 31 January 2020 doi:10.20944/preprints202001.0375.v1

Peer-reviewed version available at Appl. Sci. 2020, 10, 1994; doi:10.3390/app10061994

Table 3. Evaluation of RANs Model generated through IRIS data

Class	Precision (%)	Recall (%)	F1-Score (%)	Support
Setosa	100	100	100	5
Versicolour	83.33	100	90.91	5
Virginica	100	80	88.89	5
Avg/Total	94.44	93.33	93.26	15

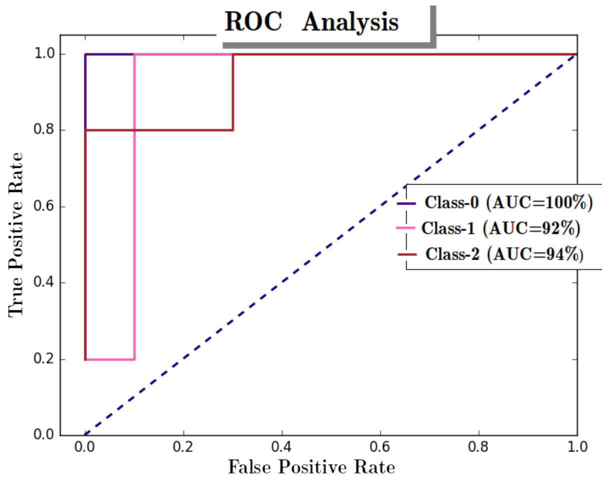

Figure 9. ROC curve analysis with IRIS dataset (having 9 : 1 *train, and test* data ratio), for Class-0 (Setosa), Class-1 (Verisicolour), and Class-2 (Virginica)

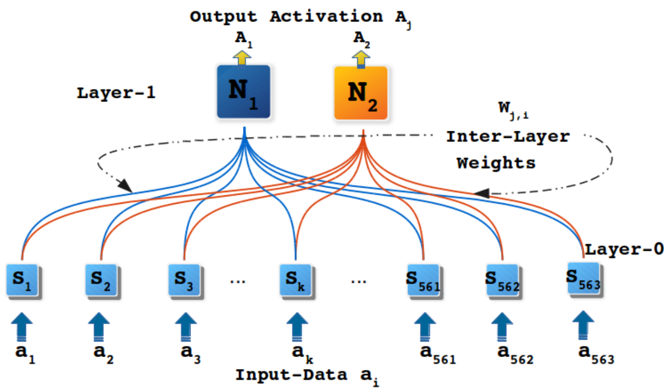

Figure 10. Model generated with RANs approach. Nodes N_1 and N_1 at Layer-1 represents either of the two Abstract Concepts, i.e. *Mobile* and *Immobile*. Each node at Layer-0 represents individual dimensions of input data vector

two layers. The K-means was configured with K=2 because the model was hypothesized to have 2 abstract concepts at Layer-1. Having fulfilled the initialization part of the CHC algorithm modeling is performed, generating a two-layered model as depicted in Figure 10. In Figure 10 Layer-0 shows *input-layer* and Layer-1 corresponds to *Abstract Concept layer* where both nodes (N_1, and N_2) represents either of the two Abstract Concepts (i.e. *Mobile* and *Immobile* Abstract Concepts).

Among captured six activities (Walking, Walking_upstairs, Walking_downstairs, Sitting, Standing and Laying), Walking, Walking_upstairs, Walking_downstairs are the actions of motion, whereas the remaining three represents static states. Based upon these two facts, we expect that one of the Abstract nodes in Layer-1 conjointly represents Walking, Walking_upstairs and Walking_downstairs as one class. The other node in Layer-1 stages the other three categories (i.e., Sitting, Standing and Laying) together. Upon performing the labeling of nodes at Layer-1 through ACL procedure (see Section A.4

Table 4. RAN's Comparative Study for UCIHAR dataset

Model	Precision (%)	Recall (%)	F1-Score (%)	Accuracy (%)
RBM	99.68 ±0.14	99.68 ±0.14	99.68 ±0.14	99.68 ±0.14
K-NN	99.96 ±0.02	99.96 ±0.02	99.96 ±0.02	99.96 ±0.02
LR	99.97 ±0.02	99.97 ±0.02	99.97 ±0.02	99.97 ±0.02
MLP	99.96 ±0.02	99.96 ±0.02	99.96 ±0.02	99.96 ±0.02
RANs	99.85 ±0.01	99.85 ±0.01	99.85 ±0.01	99.85 ±0.01
SGD	99.98 ±0.01	99.98 ±0.01	99.98 ±0.01	99.98 ±0.01

for ACL process elaboration), it was observed that Walking, Walking_upstairs, Walking_downstairs classes were mapped to one node of Layer-1. Whereas, the labels Sitting, Standing and Laying traced to the other node in Layer-1. Interestingly, this outcome commensurate with the expectations from this experiment and shows the RANs capability to identify Abstract Concepts in an unsupervised manner naturally. The True-label and Test-label obtained through ACL operation were used to form

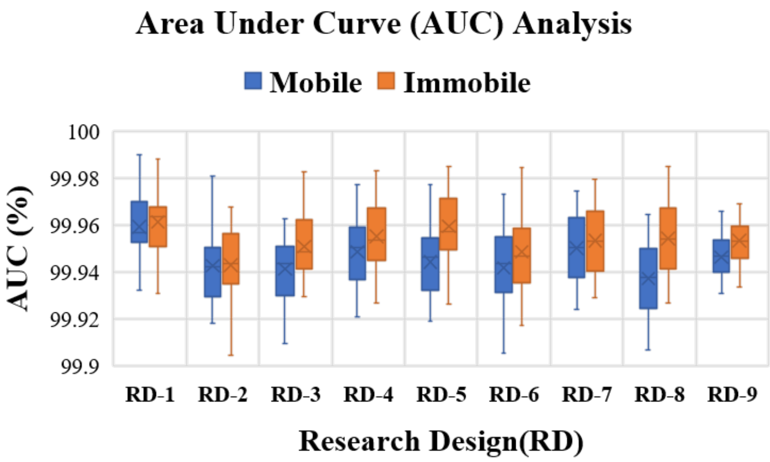

Figure 11. Area Under Curve observed during ROC curve analysis of UCIHAR data in order to determining operational points of two Abstract Concepts (i.e. *Mobile* and *Immobile*) for all nine Research Designs (RD)

the confusion matrix, which is later referred to calculate Precision, Recall, F1-Score, and Accuracy for evaluating the generated model. Node-wise binary labels and confidence scores were determined (as described in Section A.3) for both Abstract nodes at Layer-1. Figure 11 shows the Area Under Curve (AUC) observed during the ROC curve analysis of all 10-Folds in different Research Designs. With both these evaluations it is deduced that, apart from building the representation of Abstract Concepts, the model generated with RANs performed satisfactorily.

The RANs modeling was compared with five different types of approaches based upon their classification operation. To carry out the comparative study it was essential to transform the six Labels into binary Labels, because RANs modeling was identifying two Abstract Concept, and its performance was measured based upon them. Thus, with these five approaches, the Labels of the dataset were merged to form two groups, i.e., Walking, Walking_upstairs, Walking_downstairs in Class-1, and Sitting, Standing, and Laying in Class-2. Later the modeling was performed followed by validation and evaluation. Table 4 displays the comparison of all five approaches with RANs modeling. It is observed that RANs approach is competent to these five techniques, with an added advantage of being an unsupervised approach, and ability to build representations of Abstract Concepts.

5. RANs Applicability and Observations

This section highlights the scope of RANs modeling as a classifier w.r.t. distinct domains. To support this ambit of RANs usability, experimental results are reported using eight datasets concerning

 doi:10.20944/preprints202001.0375.v1

Peer-reviewed version available at Appl. Sci. 2020, 10, 1994; doi:10.3390/app10061994

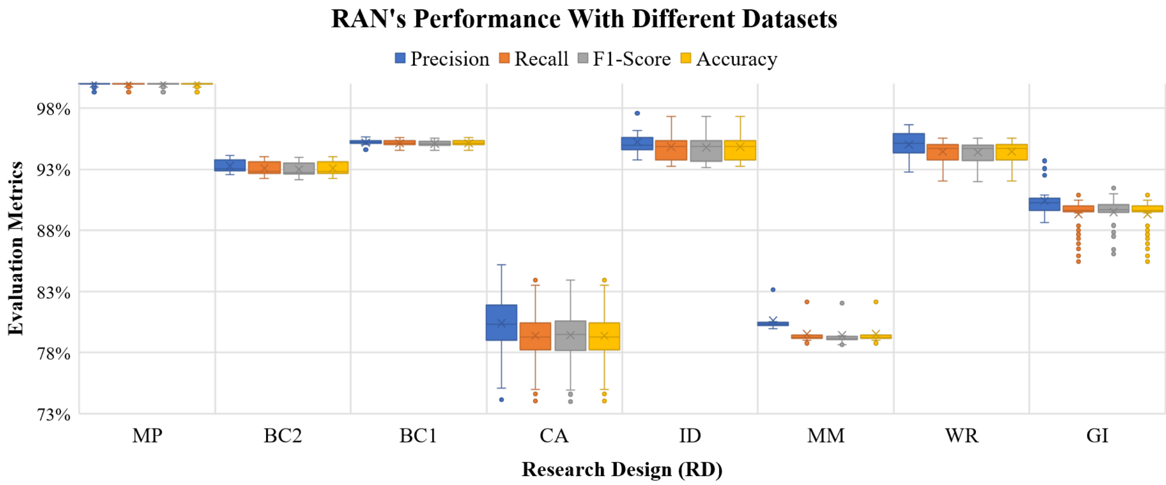

(a) RANs performance with eight different datasets depicting RANs appositeness with data belonging to distinct domains.

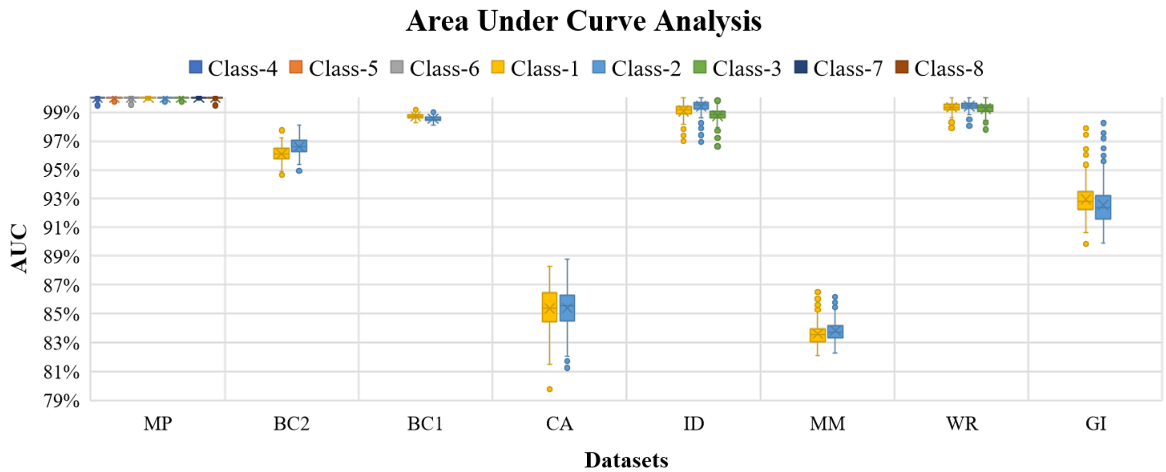

(b) Observed Area Under Curve (AUC) while performing ROC curve analysis for RANs model generated with eight different datasets.

Figure 12. RANs performance with eight datasets using Precision, Recall, F1-Score and Accuracy along with ROC-AUC analysis with Eight benchmark datasets [Mice Protein (MP), Breast Cancer 669 (BC1), Breast Cancer 569 (BC2), Credit Approval (CA), IRIS data (ID), Mamographic Mass (MM), Wine Recognition (WR) and Glass Identification (GI)]. The graph 12b shows the plot of percentage AUC for classes 1 to 8. For each dataset class labels of the graph is serially mapped as: *Mice protein* (*c-CS-s [Class-1], c-CS-m [Class-2], c-SC-s [Class-3], c-SC-m [Class-4], t-CS-s [Class-5], t-CS-m [Class-6], t-SC-s [Class-7] and t-SC-m [Class-8]*); *Mammographic Mass* (*Benign [Class-1] and Malignant [Class-2]*); *Credit Approval* (*Postitive [Class-1] and Negative [Class-2]*); *IRIS)* (*Setosa [Class-1], Versicolar [Class-2] and Verginica [Class-3]*); *Breast Cancer 569* (*Benign [Class-1] and Malignant [Class-2]*); *Breast Cancer 669* (*Benign [Class-1] and Malignant [Class-2]*), *Wine Recognition* (*Class-1, Class-2 and Class-3*) *Glass Identification* (*Window Glass [Class-1] and Non-Window Glass [Class-2]*).

Peer-reviewed version available at Appl. Sci. 2020, 10, 1994; doi:10.3390/app10061994

Table 5. RANs comparison with eight datasets belonging to different domains

Data	Algo	Precision (%)	Recall (%)	F1-Score (%)	Accuracy (%)	Data	Algo	Precision (%)	Recall (%)	F1-Score (%)	Accuracy (%)
Mice Protein	*RBM+*	43.45 ±44.07	53.50 ±38.23	45.46 ±43.36	53.50 ±38.23	**Breast Cancer 569**	*RBM+*	93.60 ± 2.69	93.51 ± 2.77	93.46 ± 2.86	93.51 ± 2.77
	KNN	98.63 ± 3.97	98.34 ± 4.84	98.07 ± 5.65	98.34 ± 4.84		*KNN*	99.80 ± 0.59	99.79 ± 0.62	99.78 ± 0.63	99.79 ± 0.62
	LR	98.99 ± 1.94	98.28 ± 3.38	98.14 ± 3.71	98.28 ± 3.38		*LR*	99.89 ± 0.07	99.89 ± 0.07	99.89 ± 0.07	99.89 ± 0.07
	MLP	98.54 ± 2.19	98.23 ± 2.71	97.83 ± 3.34	98.23 ± 2.71		*MLP*	98.67 ± 0.94	98.65 ± 0.96	98.64 ± 0.96	99.89 ± 0.07
	RAN	99.98 ± 0.06	99.97 ± 0.06	99.89 ± 0.06	99.97 ± 0.06		*RAN*	93.17 ± 0.36	92.97 ± 0.36	92.87 ± 0.42	92.97 ± 0.36
	SGD	99.11 ± 1.84	98.84 ± 2.46	98.68 ± 2.81	98.84 ± 2.46		*SGD*	99.87 ± 0.13	99.85 ± 0.18	99.83 ± 0.20	99.85 ± 0.18
Breast Cancer 669	*RBM+*	95.72 ± 3.62	95.34 ± 4.60	95.13 ± 5.16	95.34 ± 4.60	**Credit Approval**	*RBM+*	76.44 ±12.50	75.63 ±12.98	74.04 ±14.59	75.63 ±12.98
	KNN	99.46 ± 0.88	99.44 ± 0.93	99.43 ± 0.94	99.44 ± 0.93		*KNN*	95.48 ± 0.16	95.46 ± 0.17	95.46 ± 0.17	95.46 ± 0.17
	LR	99.16 ± 0.17	99.14 ± 0.17	99.15 ± 0.17	99.14 ± 0.17		*LR*	95.06 ± 0.38	95.04 ± 0.39	95.04 ± 0.39	95.04 ± 0.39
	MLP	98.96 ± 0.76	98.95 ± 0.76	98.95 ± 0.77	98.95 ± 0.76		*MLP*	98.02 ± 1.32	98.00 ± 1.34	97.99 ± 1.34	98.00 ± 1.34
	RAN	95.18 ± 0.25	95.15 ± 0.24	95.11 ± 0.25	95.15 ± 0.24		*RAN*	80.67 ± 1.37	79.58 ± 1.05	79.66 ± 1.13	79.58 ± 1.05
	SGD	99.88 ± 0.16	99.88 ± 0.16	99.18 ± 0.16	99.88 ± 0.16		*SGD*	99.77 ± 0.39	99.75 ± 0.40	99.75 ± 0.40	99.75 ± 0.40
Glass Identification	*RBM+*	82.58 ±10.29	84.19 ± 4.90	80.61 ± 8.42	84.19 ± 4.90	**Mamographic Mass**	*RBM+*	84.85 ±16.54	85.18 ±14.98	82.42 ±20.30	85.18 ±14.98
	KNN	94.08 ±12.12	95.97 ± 7.32	94.82 ±10.59	95.97 ± 7.32		*KNN*	99.65 ± 0.88	99.64 ± 0.89	99.64 ± 0.89	99.64 ± 0.89
	LR	99.52 ± 0.18	99.49 ± 0.18	99.49 ± 0.18	99.49 ± 0.18		*LR*	99.41 ± 0.30	99.40 ± 0.30	99.40 ± 0.30	99.40 ± 0.30
	MLP	93.78 ± 1.40	93.28 ± 1.52	92.85 ± 1.64	93.28 ± 1.52		*MLP*	98.91 ± 2.11	98.79 ± 2.35	98.79 ± 2.35	98.79 ± 2.35
	RAN	90.07 ± 0.43	89.18 ± 1.23	89.32 ± 1.10	89.18 ± 1.23		*RAN*	80.28 ± 0.18	79.20 ± 0.23	79.08 ± 0.24	79.20 ± 0.23
	SGD	97.95 ± 0.66	97.87 ± 0.69	97.82 ± 0.70	97.87 ± 0.69		*SGD*	99.96 ± 0.03	99.94 ± 0.07	99.93 ± 0.09	99.94 ± 0.07
IRIS	*RBM+*	79.81 ±11.91	77.41 ±11.88	70.66 ±16.28	77.41 ±11.88	**Wine Recognition**	*RBM+*	56.00 ±25.66	67.05 ±16.91	59.07 ±21.91	67.05 ±16.91
	KNN	90.41 ±28.77	92.80 ±21.61	91.00 ±27.01	92.80 ±21.61		*KNN*	90.74 ±26.00	92.88 ±19.48	91.14 ±24.70	92.88 ±19.48
	LR	97.38 ± 4.15	96.64 ± 5.65	96.45 ± 6.12	96.64 ± 5.65		*LR*	94.14 ± 1.55	93.13 ± 1.82	93.00 ± 1.92	93.13 ± 1.82
	MLP	97.31 ± 0.71	96.86 ± 1.13	96.81 ± 1.21	96.86 ± 1.13		*MLP*	97.44 ± 0.51	97.33 ± 0.59	97.32 ± 0.59	97.33 ± 0.59
	RAN	95.43 ± 0.67	95.02 ± 0.94	94.98 ± 0.98	95.02 ± 0.94		*RAN*	94.87 ± 0.91	94.34 ± 1.00	94.29 ± 1.01	94.34 ± 1.00
	SGD	94.47 ± 6.40	94.46 ± 5.20	93.31 ± 6.78	94.46 ± 5.20		*SGD*	98.13 ± 0.70	97.91 ± 0.75	97.91 ± 0.76	97.91 ± 0.75

RBM+- Restricted Boltzmann Machine + Pipelined with Logistic Regression; KNN- K Nearest Neighbor; LR- Logistic Regression; MLP- Multi Layer Perceptron; RAN- Regulated Activation Network; SGD- Stochastic Gradient Descent

with different areas. A comparative study was also carried out using these datasets to match RANs classification ability with five different classifiers.

Among the eight datasets, the *Mice Protein* [53], *Mammographic Mass* [54], *Breast Cancer 569 & 669* [55,56] data pertain to the medical field, *Glass Identification* [57] data representing forensic science, *Credit Approval* [58] represents economic data, *Iris* [59] is a botanical data, and Wine Recognition [60] is a data for chemical composition analysis. The experiments performed with these datasets were akin to the investigations done with Toy-data (in Section 3), and UCIHAR data (in Section 4.2), i.e., K-means algorithm used as concept identifier, where 'K' is the number of class labels of each dataset, the hierarchy is set to have a depth of two layers (one Input and one Abstract Concept layer). For every dataset, models were generated using thirty iterations in nine Research Designs (RD) (refer the Table A3 in Section A.2). In every RD 10-Fold cross-validation was applied to determine the performance of the models. An aggregate of Precision, Recall, F1-Score, and Accuracy of all folds in all RDs was calculated for all the datasets, as shown in Figure 12a. From the Figure 12a it can be observed that with *Mice Protein* data RANs scores 99.99%(ca.) for all evaluation metric, whereas for *Iris, Glass Identification, Breast Cancer, and Wine Recognitions* the observations were convincing, i.e., above 89.00% (ca.). In all the folds of nine RDs ROC curves were also plotted for each class label of the eight datasets, the mean AUC for each class of the datasets is shown in Figure 12b. The evaluation metrics and ROC-AUC analysis (Figure 12a & 12b respectively) displays the RANs capability in machine learning tasks with different kind of datasets.

The same procedure was applied to obtain average Precision, Recall, F1-Score and Accuracy for all the datasets with five other classifiers (i.e. *RBM+, KNN, LR, MLP, and SGD*). Table 5 shows the overall comparison. It is worth noting that being dynamic and unsupervised RANs modeling performed quite satisfactorily especially with Mice Protein data, where it outperformed SGD and RBM+, was found competent with LR, KNN and MLP classifiers. Figure 13 shows four graphs depicting RANs performance with different benchmark data sets. These graphs display an important aspect of RANs modeling and its performance behavior when evaluated to different research design 13. The Precision, Recall, F1-Score, and Accuracy trajectories of Human Activity Recognition (HAR), Breast Cancer 669 (BC1), Toy-data (TD) and Mice Protein (MP) Data is almost straight. The evaluation plots of Glass Identification (GI), Wine Recognition (WR), Mammographic Mass (MM), Breast cancer 569 (BC2) and Mice Protein (MP) datasets show a minimal decline in observations w.r.t RD-1 and RD-9 Research Design. On the contrary, results from IRIS Data (ID) and Credit Approval (CA) dataset depicted a higher value while comparing the evaluation of RD-1 with RD-9 Research Designs of these data

Peer-reviewed version available at Appl. Sci. 2020, 10, 1994; doi:10.3390/app10061994

Table 6. Feature based comparative study of RANs with 5 modeling techniques

Features\Models	RBM	K-NN	LR	MLP	RANs	SGD
Graph-Based	Yes	No	No	Yes	Yes	No
Dynamic Topology	No	No	No	No	Yes	No
Dimension Reduction	Yes	Yes	No	Yes	Yes	No
Dimension Expansion	May be	No	No	May be	Yes	No
Unisupervised	Yes	No	No	No	Yes	No
Supports Classification	Yes	Yes	Yes	Yes	Yes	Yes
Bio-inspired	Yes	No	No	Yes	Yes	No

sets. Principally, the results of all four metrics of evaluation obtained similar results (with marginal variation) irrespective of the Test and Train data ratio. This is a notable observation because it shows that RANs approach obtains a satisfactory result even when trained with a small amount of data.

Besides classification comparison, the RAN's modeling is compared with the 5 classifiers based upon 7 features: *(1)* Whether the modeling in graph based; *(2)* whether the modeling has a dynamic topology; *(3)* and *(4)* whether modeling can reduce or expand the dimension of the data; *(5)* whether modeling can perform classification; and *(7)* whether modeling is biologically inspired or not. Tabel 6 details this comparative study. It can be observed from this table that RAN is closely related to the models that are biologically inspired i.e. RBM and MLP.

6. Conclusions and Future work

To comprehend and reasoning for emotions, ideas, etc., it is evident to understand Abstract Concepts because they are perceived differently from Concrete Concepts. There have been notable efforts to study Concrete Concepts (features like walking or ingredients), but progress in investigating Abstract Concepts (generic features such as is-moving or recipe) is relatively less. This article proposes an unsupervised computational modeling approach, named Regulated Activation Networks (RANs), that has an evolving topology and learns a representation of Abstract Concepts. The RAN's methodology was exemplified through a UCI's IRIS dataset, yielding a satisfactory performance evaluation of 95% (ca.) for Precision, Recall, F1-Score and Accuracy metrics, along with an average AUC of 99% (ca.) for all the three classes in the dataset. These evaluation result not only showed the classification capability of RANs but also proved the hypothesis of the experiment i.e. the 3 newly created nodes in the Layer-1 symbolically represent the 3 classes of IRIS data as abstract concepts.

Another experiment with IRIS data displayed the characteristic of RAN's deep hierarchy generation and independence in choosing Concept Identifier. With the aid of Concept Hierarchy Creation algorithm (proposed in Section 4.1), evolving nature of RAN's modeling is shown using Affinity Propagation clustering algorithm (as an alternate Concept Identifier instead of the K-means algorithm as used in modeling with Toy-data problem). With the generated model it was shown that the model dynamically grew to a depth of six layers and performed with Precision of 94.44% (ca.), Recall of 93.33% (ca.), F1-Score of 93.26% (ca.) and Accuracy of 93.33% (ca.), along with an observed AUC of 100% (ca.), 92% (ca.) and 94% (ca.) for the three classes of data. This experiment also highlights the application of RANs modeling in data dimension transformation and data visualization.

Modeling with UCI's IoT based Home Activity Recognition (UCIHAR) smartphone sensor dataset exhibited the RAN's behavior of natural identification of generic Concepts. The experiment hypothesize that six data labels (activity of Walking, Walking_upstairs, Walking_downstairs, Sitting, Standing and Laying) of the dataset are to be identified as *Mobile* (Walking, Walking_upstairs and Walking_downstairs) and *Immobile* (Sitting, Standing and Laying) Abstract Concepts. This hypothesis was also proven using classification operation, where, the evaluation of the model shown a performance of 99.85% (ca.) for all four metrics and AUC of 99.9% (ca.) for both Abstract Concepts. The experiment also demonstrates how RAN can be used to model the data from IoT domain in an unsupervised manner.

Preprints (www.preprints.org) | NOT PEER-REVIEWED | Posted: 31 January 2020 doi:10.20944/preprints202001.0375.v1

Peer-reviewed version available at Appl. Sci. 2020, 10, 1994; doi:10.3390/app10061994

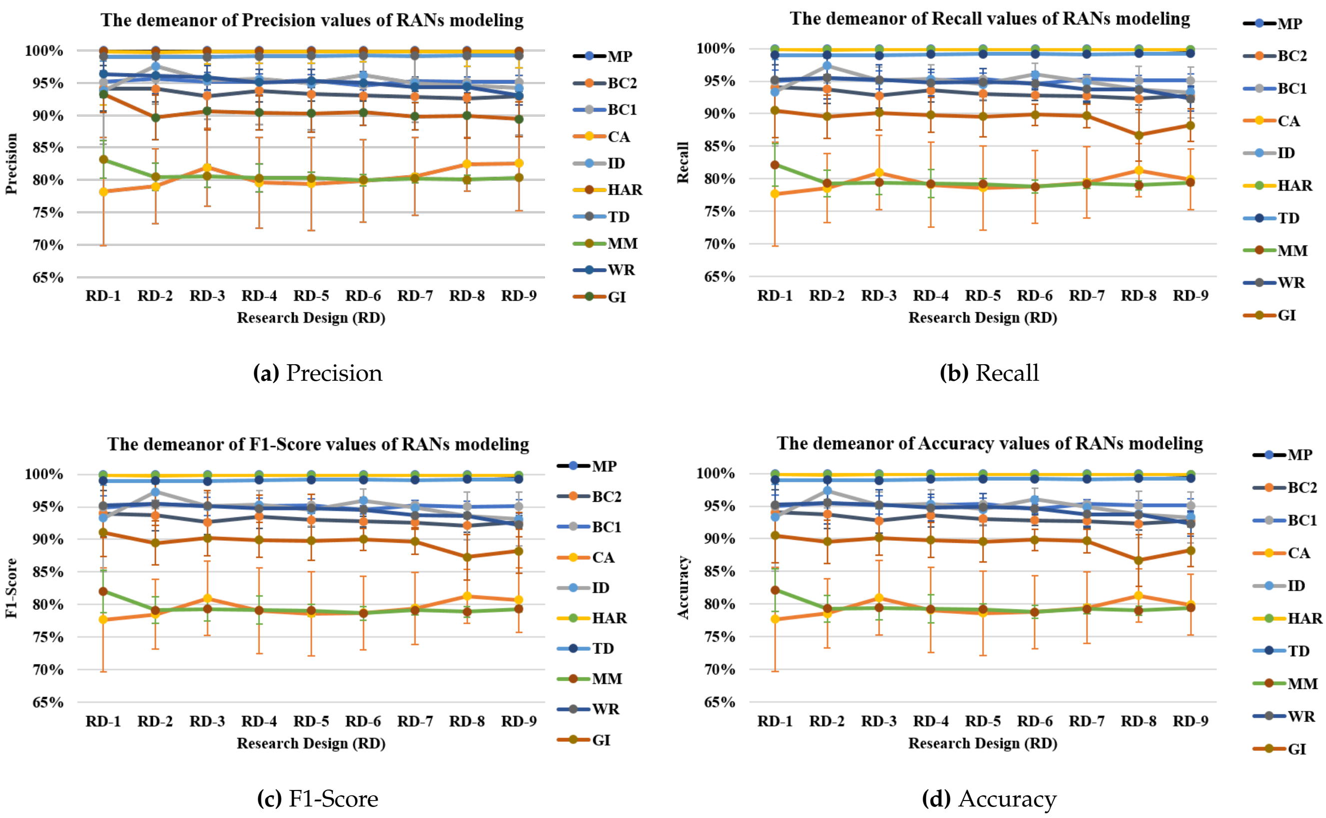

(a) Precision

(b) Recall

(c) F1-Score

(d) Accuracy

Figure 13. RANs evaluation metric (Precision, Recall, F1-Score and Acuracy) value behavior w.r.t. varying test and train data ratio over ten datasets [Mice Protein (MP), Breast Cancer 669 (BC1), Breast Cancer 569 (BC2), Credit Approval (CA), IRIS data (ID), Mamographic Mass (MM), Human Activity Recognition (HAR), Toy-data(TD), Wine Recognition (WR) and Glass Identification (GI)].

Peer-reviewed version available at Appl. Sci. 2020, 10, 1994; doi:10.3390/app10061994

Table 7. Acronyms used in the Article

Acronym	Description	Acronym	Description	Acronym	Description
ACL	Abstract Concept Labeling	DoC	Degree of Confidence	MM	Mammography Mass Dataset
AUC	Area Under Curve	GDF	Geometric Distance Function	MP	Mice Protein Dataset
BC1	Breast Cancer 669 Dataset	GI	Glass Identification Dataset	MRI	Magnetic Resonance Imaging
BC2	Breast Cancer 569 Dataset	HAR	Human Activity Recognition Data	RANs	Regulated Activation Networks
CA	Credit Approval Dataset	ID	IRIS Dataset	RBM	Restricted Boltzmann Machine
CC	Concept Creation	ILL	Inter Layer Learning	RD	Research Design
CHC	Concept Hierarchy Creation	ILW	Inter Layer Weights	ROC	Receiver Operating Characteristic
CI	Concept Identification	K-NN	K Nearest Neighbor	SGD	Stochastic Gradient Descent
CLS	Current Layer Size	LR	Logistic Regression	STF	Similarity Translation Function
CRDP	Cluster Representative Data Point	MLP	Multilayer Perceptron	UAP	Upward Activation Propagation

The proof of concept of RAN's modeling as a Machine Learning classifier was also provided with eight UCI benchmarks. It was identified that RAN's approach performed satisfactorily displaying the best outcome of 98.9% (ca.) with *Mice Protein* dataset (for all metrics). The comparison of RAN's modeling with five classifiers substantiated the effectiveness of the proposed methodology. We also observed that the RAN's performance remained similar irrespective of the size of train data. RAN was also compared with the 5 classifiers based upon its features and it was observed that RAN was similar to bio-inspired models. During the simulations, a non-convexity was observed in several datasets. As future work, we intend to improve RAN's modeling that can capture the non-convexity in the data and enhance the modeling to build non-convex abstract concepts.

Funding: "The work presented in this paper was partially carried out in the scope of the SOCIALITE Project (PTDC/EEI-SCR/2072/2014), co-financed by COMPETE 2020, Portugal 2020 - Operational Program for Competitiveness and Internationalization (POCI), European Union's ERDF (European Regional Development Fund), and the Portuguese Foundation for Science and Technology (FCT).

Conflicts of Interest: "The authors declare no conflict of interest."

Abbreviations

The abbreviations are used in this manuscript are listed in Table 7:

Appendix A Supplementary Materials

Appendix A.1 Data & Scripts

This section provides links to download the data and python script used to perform RANs modeling experiments, mentioned in this article. The data and script folders can be downloaded from the web URL mentioned in Table A1. The data folder contains many files and the direct path to the files are provided in the Table A1. Similarly, the script folder *RAN_V2.0* also contains many folders where Folder *RAN* consist of the python scripts. The folder *Observations* is for storing the outcome of the experiments, at the beginning of each experiment the empty folder in directory *empty_passes_for_Experiment_Observations* must be copied into the *Observation* directory. The python script related to RANs modeling is in folder *RAN*, the description is mentioned in the Table A1.

The implemented RANs modeling tool in python takes input data in a specific format (shown in Table A2). Besides the data, the inputs require a header as the first row stacked over the original data. Each header element, $[H-1, H-2, ..., H-n]$, is the Maximum value possible for their respective column (feature, or dimension). It is assumed that the minimum value of the column is zero, if it is not then the data must be transformed between zero and the maximum positive value as described in Section 3.

Preprints (www.preprints.org) | NOT PEER-REVIEWED | Posted: 31 January 2020 doi:10.20944/preprints202001.0375.v1

Peer-reviewed version available at *Appl. Sci.* **2020**, *10*, 1994; doi:10.3390/app10061994

Table A1. Data and Python Script of RANs modeling

Type	Description	File-path
Data	Download link	https://www.dropbox.com/sh/3410ozeru3o5opm/AAA24aUGtUS1i7xHKp9kyzRKa?dl=0
	IRIS Data	data/iris_with_label.csv
	Mice Protein data	data/Data_cortex_Nuclear/mice_with_class_label.csv
	Glass Identification data	data/newDataToExplore/new/GlassIdentificationDatabase/RANsform.csv
	Wine Recognition data	data/newDataToExplore/new/WineRecognitionData/RansForm.csv
	Breast cancer 669 data	data/newDataToExplore/new/breastCancerDatabases/699RansForm.csv
	Breast Cancer 559 data	data/newDataToExplore/new/breastCancerDatabases/569RansForm.csv
	UCIHAR data	data/UCI_HAR_Dataset.csv
	Mamographic Mass data	data/newDataToExplore/new/MammographicMassData/RansForm1
	Credit Approval data	data/newDataToExplore/new/CreditApproval/RansForm.csv
	Toy-data data	data/toydata5clustersRAN.csv
Script	Download Link	https://www.dropbox.com/sh/rcw1cj4ce1f3zic/AAAm6wVTj2qsLZ1lbc3kn4MPa?dl=0
	RANs classes and methods	RAN_V2-0/RAN/RAN_kfold.py
	Methods	RAN_V2-0/RAN/Layer.py
	Utilities like Labeling and plotting	RAN_V2-0/RAN/UtilsRAN.py
	Python Script for using RANs	RAN_V2-0/RAN/RAN_input_T1.py

Table A2. Input Data Format for implemented RANs Modeling

Header	**H-1**	**H-2**	**.............**	**H-n**
Data Instances	D-1	D-2	....	D-n
	D-1	D-2	....	D-n
	.	.	....	.
	.	.	....	.
	.	.	....	.
	D-1	D-2	....	D-n

Appendix A.2 Model Configurations and Research Design

Various experiments, reported in this article, were conducted with several datasets, using six modeling techniques including the proposed methodology i.e. RANs modeling. Table A4 in Section A.2 shows configurations of all the models for all the experiments. The experiments were carried out using python programing language, and implementations of Restricted Boltzmann Machine pipelined with Logistic Regression (RBM+), Logistic Regression (LR), K-Nearest Neighbor (K-NN), Multilayer Perceptron (MLP), and Stochastic Gradient Descent (SGD) models of Scikit-learn library [**?**]. It is to be noted that experiments with RBM were carried out, pipelined with the LR algorithm using the default configuration of its implementation in scikit-learn library. The Table A3 lists the nine Research Designs (RD) used in the experiments of this article. In every RD the ratio of the Train and Test data is varied to capture the ability of the classifier being inspected. The Table 7 lists the acronyms used in this article.

Appendix A.3 Multi-class ROC analysis with RANs Modeling

This study is carried out by two processes, first the input true-labels are transformed into a separate vector of binary labels, individually for all Abstract nodes (i.e. 1 for class c1, 0 for all other classes), second, calculating the confidence score for each instance of the input data (or test-data). Both processes are described as follows:

1 **Node-wise binary transformation of True-Labels**: For example, suppose there are three classes (c1, c2, c3) represented by three abstract nodes (n1, n2, and n3) in RANs model at Layer-1, and

Table A3. Train & Test data distributions in nine Research Designs (RD)

RD-1		**RD-2**		**RD-3**		**RD-4**		**RD-5**	
Train	*Test*	*Train*	*Test*	*Train*	*Test*	*Train*	*Test*	*Train*	*Test*
90%	10%	80%	20%	70%	30%	60%	40%	50%	50%
RD-1		**RD-7**		**RD-8**		**RD-9**		————	
Train	*Test*	*Train*	*Test*	*Train*	*Test*	*Train*	*Test*	——	——
40%	60%	30%	70%	20%	80%	10%	90%	——	——

Preprints (www.preprints.org) | NOT PEER-REVIEWED | Posted: 31 January 2020 doi:10.20944/preprints202001.0375.v1

Peer-reviewed version available at *Appl. Sci.* **2020**, *10*, 1994; doi:10.3390/app10061994

Table A4. Dataset specific configuration details of models

Data	Algo	Configurations	Data	Algo	Configurations
Toy-data	*RBM + LR*	Lr=0.000001, iter=500, comp=20 max_iter=30, C=70	**UCIHAR**	*RBM + LR*	Lr=0.06, iter=500, comp=10 max_iter=10, C=1
	K-NN	n_neighbors=30		*K-NN*	n_neighbors= 15
	LR	max_iter=10, C=1		*LR*	max_iter=30, C=1
	MLP	Rs=1, hls=10, iter=250		*MLP*	Rs=1, hls=10, iter=400
	RANs	CLS=5, Desired_depth=1		*RANs*	CLS=2, Desired_depth=1
	SGD	alpha=0.0001, n_iter=5, epsilon=0.25		*SGD*	alpha=0.1, n_iter=10, epsilon=0.25
Mice Protein	*RBM + LR*	Lr=0.1, iter=500, comp=20 max_iter=30, C=30	**Breast Cancer 569**	*RBM + LR*	Lr=0.006, iter=100, comp=10 max_iter=30, C=1
	K-NN	n_neighbors=15		*K-NN*	n_neighbors=30
	LR	max_iter=4, C=0.00001		*LR*	max_iter=10, C=0.001
	MLP	Rs=1, hls=10, iter=300		*MLP*	Rs=1, hls=10, iter=200
	RANs	CLS=8, Desired_depth=1		*RANs*	CLS=2, Desired_depth=1
	SGD	alpha=0.1, n_iter=10, epsilon=0.25		*SGD*	alpha=,0.0001 n_iter=5, epsilon=0.25
Breast Cancer 669	*RBM + LR*	Lr=0.001, iter=100, comp=10 max_iter=30, C=1	**Credit Approval**	*RBM + LR*	Lr=0.006, iter=100, comp=10 max_iter=30, C=1
	K-NN	n_neighbors=10		*K-NN*	n_neighbors=30
	LR	max_iter=10, C=0.001		*LR*	max_iter=10, C=0.001
	MLP	Rs=1, hls=10, iter=200		*MLP*	Rs=1, hls=10, iter=200
	RANs	CLS=2, Desired_depth=1		*RANs*	CLS=2, Desired_depth=1
	SGD	alpha=0.0001, n_iter=5, epsilon=0.25		*SGD*	alpha=0.0001, n_iter=5, epsilon=0.25
Glass Identification	*RBM + LR*	Lr=0.001, iter=400, comp=10 max_iter=30, C=5	**Mamographic Mass**	*RBM + LR*	Lr=0.01, iter=500, comp=20 max_iter=30, C=5
	K-NN	n_neighbors=15		*K-NN*	n_neighbors=30
	LR	max_iter=5, C=0.00001		*LR*	max_iter=5, C=1
	MLP	Rs=1, hls=10, iter=200		*MLP*	Rs=1, hls=10, iter=250
	RANs	CLS=2, Desired_depth=1		*RANs*	CLS=2, Desired_depth=1
	SGD	alpha=0.01, n_iter=10, epsilon=0.25		*SGD*	alpha=0.0001, n_iter=5, epsilon=0.25
IRIS	*RBM + LR*	Lr=0.01, iter=1000, comp=20 max_iter=30, C=5	**Wine Recognition**	*RBM + LR*	Lr=0.01, iter=500, comp=20 max_iter=30, C=50
	K-NN	n_neighbors=15		*K-NN*	n_neighbors=15
	LR	max_iter=10, C=1		*LR*	max_iter=10, C=0.01
	MLP	Rs=1, hls=10, iter=400		*MLP*	Rs=1, hls=10, iter=300
	RANs	CLS=3, Desired_depth=1		*RANs*	CLS=3, Desired_depth=1
	SGD	alpha=0.01, n_iter=10, epsilon=0.25		*SGD*	alpha=0.01, n_iter=10, epsilon=0.25
Lr-Learning Rate; iter-Iterations; comp-Number of Hidden Components of RBM; RS-Random State hls=Hidden Layer Sizes; CLS-Number of clusters at the input layer of RANs					

let true-label be [c1, c2, c2, c1, c2, c3, c3] for 7 test instances, then for node n1 label will be [1, 0, 0, 1, 0, 0, 0] where 1 represents class c1, and 0 depicts others (i.e. c2, and c3).

2 **Node-wise confidence-score calculation**: This is calculated by averaging activation-value and confidence-indicator of activation for an input instance at an Abstract node. Activation-value is an individual activation of an activation vector obtained by propagating up the data using UAP mechanism of RANs whereas, confidence-indicator is calculated by min-max normalization operation of activation vector. For example, after UAP operation each node (n1, n2, and n3) receives activation [0.89, 0.34, 0.11] (a vector of activation), and confidence-indicator is min-max ([0.89, 0.34, 0.11]) = [1.0, 0.29, 0.0]. and the confidence-score for nodes n1= (0.89 + 1.0)/2.0 = 0.95, n2= (0.34 + 0.29)/2.0 = 0.32, and n3= (0.11 + 0.11)/2.0 = 0.05.

Appendix A.4 Abstract Concept Labeling (ACL)

This method is optional and useful when the input data is labeled. With this mechanism, we associate an identifier to every Abstract Concept node N_j. Having generated the RANs model with CI, then trough CC, ILL, input data is sorted label-wise, and perform UAP operation. The propagated data is inspected class-wise, and label node N_j with a class-name for which it got the maximum count of

Preprints (www.preprints.org) | NOT PEER-REVIEWED | Posted: 31 January 2020 doi:10.20944/preprints202001.0375.v1

Peer-reviewed version available at Appl. Sci. 2020, 10, 1994; doi:10.3390/app10061994

the highest activation. For example, suppose input data for class-X has 100 instances, after inspecting the propagated data, it is observed that node N_1 received highest activation 74-times, whereas, with remaining 26 cases other nodes experienced maximum activation, therefore, we recognize node N_1 as representative of class-X. *True-Labels* are identified by mapping each class of the input instance directly to its respective node representative *Observed-Labels* are obtained by propagating every test-instance through UAP operation, inspecting which Abstract node received the highest activation for that data-unit, and label it with the class represented by that node. True-Labels and Observed-Labels are used to validate the model's performance.

References

1. Kiefer, M.; Pulvermüller, F. Conceptual representations in mind and brain: theoretical developments, current evidence and future directions. *Cortex* **2012**, *48*, 805–825.
2. Xiao, P.; Toivonen, H.; Gross, O.; Cardoso, A.; Correia, J.a.; Machado, P.; Martins, P.; Oliveira, H.G.; Sharma, R.; Pinto, A.M.; Díaz, A.; Francisco, V.; Gervás, P.; Hervás, R.; León, C.; Forth, J.; Purver, M.; Wiggins, G.A.; Miljković, D.; Podpečan, V.; Pollak, S.; Kralj, J.; Žnidaršič, M.; Bohanec, M.; Lavrač, N.; Urbančič, T.; Velde, F.V.D.; Battersby, S. Conceptual Representations for Computational Concept Creation. *ACM Computing Survey* **2019**, *52*, 1–33.
3. Anderson, J.R.; Matessa, M.; Lebiere, C. ACT-R: A theory of higher level cognition and its relation to visual attention. *Human-Computer Interaction* **1997**, *12*, 439–462.
4. Gärdenfors, P. *Conceptual spaces: The geometry of thought*; MIT press, 2004.
5. Sun, R.; Peterson, T. Learning in reactive sequential decision tasks: The CLARION model. IEEE International Conference on Neural Networks. IEEE, 1996, Vol. 2, pp. 1073–1078.
6. Rumelhart, D.E.; Hinton, G.E.; Williams, R.J. Learning internal representations by error propagation. Technical report, California Univ San Diego La Jolla Inst for Cognitive Science, 1985.
7. Freedman, D.A. *Statistical models: theory and practice*; Cambridge University Press, 2009; chapter 7.
8. Altman, N.S. An introduction to kernel and nearest-neighbor nonparametric regression. *The American Statistician* **1992**, *46*, 175–185.
9. Zhang, T. Solving large scale linear prediction problems using stochastic gradient descent algorithms. Proceedings of the twenty-first international conference on Machine learning. ACM, 2004, p. 116.
10. Hinton, G. A practical guide to training Restricted Boltzmann Machines. *Momentum* **2010**, *9*, 926.
11. Binder, J.R.; Westbury, C.F.; McKiernan, K.A.; Possing, E.T.; Medler, D.A. Distinct brain systems for processing concrete and abstract concepts. *Journal of Cognitive Neuroscience* **2005**, *17*, 905–917.
12. Gao, C.; Baucom, L.B.; Kim, J.; Wang, J.; Wedell, D.H.; Shinkareva, S.V. Distinguishing Abstract from Concrete concepts in Supramodal Brain Begions. *Neuropsychologia* **2019**, *131*, 102 – 110.
13. Kousta, S.T.; Vigliocco, G.; Vinson, D.P.; Andrews, M.; Del Campo, E. The representation of abstract words: Why emotion matters. *Journal of Experimental Psychology: General* **2011**, *140*, 14.
14. Barsalou, L.W.; Wiemer-Hastings, K. Situating abstract concepts. *Grounding cognition: The role of perception and action in memory, language, and thought* **2005**, pp. 129–163.
15. Löhr, G. Embodied cognition and abstract concepts: Do concept empiricists leave anything out? *Philosophical Psychology* **2019**, *32*, 161–185.
16. Gibbs Jr, R.W. Why many concepts are metaphorical. *Cognition* **1996**, *61*, 309–319.
17. Hill, F.; Korhonen, A. Learning Abstract Concept Embeddings from Multi-Modal Data: Since You Probably Can't See What I Mean. Empirical Methods in Natural Language Processing, 2014, pp. 255–265.
18. Iosif, E.; Potamianos, A.; Giannoudaki, M.; Zervanou, K. Semantic similarity computation for abstract and concrete nouns using network-based distributional semantic models. Proceedings of the 10th International Conference on Computational Semantics. Potsdam, Germany:[sn], 2013, pp. 328–334.
19. Iosif, E. Network-based distributional semantic models. PhD thesis, Technical University of Crete, Chania, Greece, 2013.
20. Maniezzo, V. Genetic evolution of the topology and weight distribution of neural networks. *IEEE Transactions on Neural Networks* **1994**, *5*, 39–53.
21. Stanley, K.O.; Miikkulainen, R. Evolving neural networks through augmenting topologies. *Evolutionary computation* **2002**, *10*, 99–127.

22. Miikkulainen, R.; Liang, J.; Meyerson, E.; Rawal, A.; Fink, D.; Francon, O.; Raju, B.; Shahrzad, H.; Navruzyan, A.; Duffy, N.; others. Evolving deep neural networks. In *Artificial Intelligence in the Age of Neural Networks and Brain Computing*; Elsevier, 2019; pp. 293–312.
23. Hintze, A.; Edlund, J.A.; Olson, R.S.; Knoester, D.B.; Schossau, J.; Albantakis, L.; Tehrani-Saleh, A.; Kvam, P.; Sheneman, L.; Goldsby, H.; others. Markov Brains: A technical introduction. *arXiv preprint arXiv:1709.05601* **2017**.
24. Pinto, A.M.; Barroso, L. Principles of Regulated Activation Networks. In *Graph-Based Representation and Reasoning*; Springer, 2014; pp. 231–244.
25. Jacoby, L. Perceptual enhancement: persistent effects of an experience. *Journal of Experimantal Psychology. Learning, Memmory and Cognition* **1983**, *9*, 21–38.
26. Roediger, H.; Blaxton, T. Effects of varying modality, surface features, and retention interval on priming in word-fragment completion. *Memory & Cognition* **1987**, *15*, 379–388.
27. Roediger, H.; Mcdermott, K. Creating false memories: Remembering words not presented in lists. *Journal of Experimental Psychology. Learning, Memory, and Cognition* **1995**, *21*, 803–814.
28. Gärdenfors, P. Conceptual spaces as a framework for knowledge representation. *Mind and Matter* **2004**, *2*, 9–27.
29. Sivik, L.; Taft, C. Color naming: A mapping in the IMCS of common color terms. *Scandinavian Journal of Psychology* **1994**, *35*, 144–164.
30. Rosch, E. Cognitive representations of semantic categories. *Journal of Experimental Psychology: General* **1975**, *104*, 192.
31. Mervis, C.B.; Rosch, E. Categorization of natural objects. *Annual Review of Psychology* **1981**, *32*, 89–115.
32. Rosch, E. Prototype classification and logical classification: The two systems. *New trends in conceptual representation: Challenges to Piaget's theory* **1983**, pp. 73–86.
33. Parsons, L. Evaluating subspace clustering algorithms. in Workshop on Clustering High Dimensional Data and its Applications, SIAM International Conference on Data Mining, 2004, pp. 48–56.
34. Livingstone, D. *Unsupervised Learning*; John Wiley & Sons, Ltd, 2009; pp. 119–144.
35. Yoon, J.; Raghavan, V.; Chakilam, V. BitCube: clustering and statistical analysis for XML documents. *Journal of Intelligent Information Systems* **2001**.
36. Van Deursen, A.; Kuipers, T. Identifying Objects Using Cluster and Concept Analysis. Proceedings of the 21st International Conference on Software Engineering. ACM, 1999, pp. 246–255.
37. LeCun, Y.; Bengio, Y.; Hinton, G. Deep learning. *Nature* **2015**, *521*, 436–444.
38. Schmidhuber, J. Deep Learning in Neural Networks: An Overview. *Neural Networks* **2015**, *61*, 85–117. Published online 2014; based on TR arXiv:1404.7828 [cs.NE].
39. Bengio, Y. Learning Deep Architectures for AI. *Foundations and Trends® in Machine Learning* **2009**, *2*, 1–127.
40. Eigen, D.; Rolfe, J.; Fergus, R.; LeCun, Y. Understanding Deep Architectures using a Recursive Convolutional Network. International Conference on Learning Representations. CBLS, 2014.
41. Bengio, Y.; Courville, A.; Vincent, P. Representation Learning: A Review and New Perspectives. *IEEE Transactions on Pattern Analysis and Machine Intelligence* **2013**, *35*, 1798–1828.
42. Anderson, J. A spreading activation theory of memory. *Journal of Verbal Learning and Verbal Behavior* **1983**, *22*, 261–295.
43. Collins, A.; Quillian, M. Retrieval time from semantic memory. *Journal of Verbal Learning and Verbal Behavior* **1969**, *8*, 240 – 247.
44. Crestani, F. Application of Spreading Activation Techniques in Information Retrieval. *Artificial Intelligence Review* **1997**, *11*, 453–482.
45. McNamara, T.; Altarriba, J. Depth of spreading activation revisited: Semantic mediated priming occurs in lexical decisions. *Journal of Memory and Language* **1988**, *27*, 545 – 559.
46. Roediger, H.; Balota, D.; Watson, J. Spreading activation and arousal of false memories. *The nature of remembering: Essays in honor of Robert G. Crowder* **2001**, pp. 95–115.
47. Kavukcuoglu, K.; Sermanet, P.; Boureau, Y.; Gregor, K.; Mathieu, M.; LeCun, Y. Learning Convolutional Feature Hierachies for Visual Recognition. Advances in Neural Information Processing Systems (NIPS 2010), 2010, Vol. 23.

Peer-reviewed version available at *Appl. Sci.* **2020**, *10*, 1994; doi:10.3390/app10061994

48. Sermanet, P.; Eigen, D.; Zhang, X.; Mathieu, M.; Fergus, R.; LeCun, Y. OverFeat: Integrated Recognition, Localization and Detection using Convolutional Networks. International Conference on Learning Representations. CBLS, 2014.
49. Hartigan, J.A.; Wong, M.A. Algorithm AS 136: A K-means Clustering Algorithm. *Journal of the Royal Statistical Society. Series C (Applied Statistics)* **1979**, *28*, 100–108.
50. Frey, B.J.; Dueck, D. Clustering by Passing Messages Between Data Points. *Science* **2007**, *315*, 972–976.
51. Lichman, M. UCI Machine Learning Repository, 2013.
52. Anguita, D.; Ghio, A.; Oneto, L.; Parra, X.; Reyes-Ortiz, J.L. A Public Domain Dataset for Human Activity Recognition using Smartphones. Empirical Methods in Natural Language Processing, 2013.
53. Higuera, C.; Gardiner, K.J.; Cios, K.J. Self-organizing feature maps identify proteins critical to learning in a mouse model of down syndrome. *PLOS ONE* **2015**, *10*, e0129126.
54. Elter, M.; Schulz-Wendtland, R.; Wittenberg, T. The prediction of breast cancer biopsy outcomes using two CAD approaches that both emphasize an intelligible decision process. *Medical Physics* **2007**, *34*, 4164–4172.
55. Street, W.N.; Wolberg, W.H.; Mangasarian, O.L. Nuclear feature extraction for breast tumor diagnosis. Biomedical Image Processing and Biomedical Visualization. International Society for Optics and Photonics, 1993, Vol. 1905, pp. 861–871.
56. Bennett, K.P.; Mangasarian, O.L. Robust linear programming discrimination of two linearly inseparable sets. *Optimization methods and software* **1992**, *1*, 23–34.
57. Evett, I.W.; Spiehler, E.J. Rule induction in forensic science. Technical report, Central Research Establishment, Home Office Forensic Science Service, 1987.
58. Quinlan, J.R. Simplifying decision trees. *International Journal of Human-Computer Studies* **1999**, *51*, 497–510.
59. Fisher, R.A. The use of multiple measurements in taxonomic problems. *Annals of Human Genetics* **1936**, *7*, 179–188.
60. Forina, M.; Leardi, R.; Armanino, C.; Lanteri, S.; Conti, P.; Princi, P. PARVUS: An extendable package of programs for data exploration, classification and correlation. *Journal of Chemometrics* **1988**, *4*, 191–193.